AGU PUBLICATIONS

Paleoceanography

RESEARCH ARTICLE
10.1002/2014PA002623

Timing of the descent into the last Ice Age determined by the bipolar seesaw

Stephen Barker[1] and Paula Diz[2]

[1]School of Earth and Ocean Sciences, Cardiff University, Cardiff, UK, [2]Department of Xeociencias Mariñas e Ordenación do TerritorioFacultade de Ciencias do Mar, University of Vigo, Vigo, Spain

Key Points:
- Southern end of the instantaneous bipolar seesaw observed during MIS 3-2
- Descent into glacial MIS 4 displayed interhemispheric synchrony
- Bipolar seesaw plays a role in interglacial to glacial transitions

Supporting Information:
- Readme
- Data S1
- Text S1

Correspondence to:
S. Barker,
Barkers3@cardiff.ac.uk

Citation:
Barker, S., and P. Diz (2014), Timing of the descent into the last Ice Age determined by the bipolar seesaw, *Paleoceanography*, *29*, 489–507, doi:10.1002/2014PA002623.

Received 28 JAN 2014
Accepted 9 MAY 2014
Accepted article online 14 MAY 2014
Published online 11 JUN 2014

Abstract We present planktonic foraminiferal fauna and isotope records from the SE Atlantic that highlight the nature of millennial-scale variability over the last 100 kyr. We derive a hypothesis-driven age model for our records based on the empirical link between variations in Greenland temperature, ocean circulation, and carbonate preservation in the deep SE Atlantic. Our results extend earlier findings of an antiphase (seesaw) relationship between north and south for the largest abrupt events of Marine Isotope Stage (MIS) 3–2 and the last deglaciation. In particular, we find that Heinrich Stadials were paralleled by inferred southward shifts of the thermal Subtropical Front. These were followed by pronounced rebounds of the front with the return to interstadial conditions in the north. Our results also shed light on the mechanism of glaciation. In contrast to the last deglaciation, which was a globally symmetric change superposed by interhemispheric asynchronicity, we find that the descent into full glacial conditions at the onset of MIS 4 (~70 ka) displayed interhemispheric synchrony. We suggest that this globally synchronous descent into glacial MIS 4 was preconditioned by orbital changes, but the timing was ultimately determined by abrupt changes in ocean/atmosphere circulation patterns i.e., the bipolar seesaw.

1. Introduction

It is commonly argued that Earth's glacial cycles are driven by changes in orbital geometry [*Imbrie et al.*, 1993], but it is also acknowledged that nonlinearities and feedbacks within the climate system are required in order to explain the precise timing and magnitude of climatic change that is observed [*Broecker and Denton*, 1989; *Imbrie et al.*, 1993]. Much attention has been paid to the mechanisms associated with glacial terminations (the transitions from glacial to interglacial state), and the recent observation of a ubiquitous association between abrupt climate oscillations (involving the so-called bipolar seesaw [*Crowley*, 1992; *Broecker*, 1998; *Stocker and Johnsen*, 2003]) and glacial terminations of the Late Pleistocene [*Cheng et al.*, 2009; *Barker et al.*, 2011] has bolstered suggestions [*Mix et al.*, 1986; *Broecker and Denton*, 1989] that abrupt reorganizations of the ocean-atmosphere system might play an active role in deglaciation. The fact that interglacial to glacial (IG-G) transitions are also associated with enhanced millennial-scale climate variability [*Sima et al.*, 2004; *Barker et al.*, 2011] begs the question as to whether or not such variability might also play an active role in glacial development. Here we present new records from the SE Atlantic that we argue provide evidence for an active role of the bipolar seesaw in the most recent IG-G transition.

1.1. Millennial-Scale Variability During the Last Glacial Period

The asynchronous relationship, both inferred [*Charles et al.*, 1996] and observed [*Blunier et al.*, 1998; *Blunier and Brook*, 2001], between millennial-scale events in ice core temperature records from Greenland and Antarctica stimulated debate as to whether changes in the south led those in the north or vice versa [*Blunier et al.*, 1998; *Steig and Alley*, 2002; *Schmittner et al.*, 2003; *Huybers*, 2004]. While temperature records from Greenland revealed the well-known Dansgaard-Oeschger (D-O) oscillations, a series of large (>10°C) and abrupt (decadal) shifts between cold (stadial) and warmer (interstadial) episodes, the Antarctic records showed a very different picture, with changes occurring more gradually and approximately out-of-phase with those in the north. More specifically, Antarctic temperatures increased during northern stadial events and decreased during interstadials. At first [*Charles et al.*, 1996], this asynchronous relationship seemed to rule out ocean circulation as a driver of bipolar temperature variations, either by positive reinforcement, whereby increased production of deep water in the North Atlantic would warm both the north and south in symmetry [*Weyl*, 1968], or through the bipolar seesaw, whereby changes in the northward heat transport associated

with the Atlantic Meridional Overturning Circulation (AMOC) would drive opposite changes in either hemisphere [*Crowley*, 1992].

Later studies provided some reconciliation of this problem by invoking contrasting timescales for the processes governing temperature change over Greenland and Antarctica. By calling on the large thermal inertia of (for example) the Southern Ocean, a reduction in the AMOC (or more precisely northward heat transport) could lead to an abrupt cooling over Greenland with a more gradual warming over Antarctica (and vice versa) [*Ganopolski and Rahmstorf*, 2001; *Schmittner et al.*, 2003; *Stocker and Johnsen*, 2003]. Accordingly, the relationship between bipolar ice core temperature records could be conveniently described by a conceptual model known as the thermal bipolar seesaw [*Stocker and Johnsen*, 2003], which predicted an inverse relationship between the rate of change of Antarctic temperature and the temperature anomaly over Greenland [*Barker et al.*, 2011]. The actual north-south relationship may therefore be considered as purely antiphase [*Hinnov et al.*, 2002; *Ganopolski and Roche*, 2009; *Barker et al.*, 2011].

One of the key predictions of the thermal bipolar seesaw is the existence of a direct counterpart to the abrupt variability recorded over Greenland in the South Atlantic-Southern Ocean (SASO) region [see *Stocker and Johnsen*, 2003, Figure 2] (we refer to the antiphasing between Greenland and the SASO as the "instantaneous bipolar seesaw" [*Barker et al.*, 2009] to distinguish it from the time-integrated relationship between Greenland and Antarctica). Our initial findings in the SE Atlantic [*Barker et al.*, 2009] suggested that abrupt shifts in the latitudinal position of the thermal Subtropical Front could represent this counterpart, providing direct evidence for the predicted interhemispheric phasing [*Severinghaus*, 2009]. Here we extend these records back to 100 ka.

1.2. Orbital Timescales

A long standing question in paleoclimate research (and a fly in the ointment for Milankovitch Theory according to *Mercer* [1984]) concerns the interhemispheric symmetry of glacial cycles, given that the commonly assumed driver, summer solar radiation, varies in an asymmetric sense between north and south [*Huybers*, 2009]. In particular, glacial cycles apparently follow variations in northern summer radiation, leaving the southern variations essentially unexplained. The situation is further complicated by an apparent lead of southern changes over those in the north on a variety of timescales [*Imbrie et al.*, 1992; *Sowers and Bender*, 1995; *Charles et al.*, 1996; *Petit et al.*, 1999; *Blunier and Brook*, 2001; *Wunsch*, 2003]. On the other hand, it has been suggested that the systematic superposition of millennial-scale perturbations on longer-term variations can give rise to apparent leads and lags on orbital timescales [*Alley et al.*, 2002; *Ganopolski and Roche*, 2009; *Ziegler et al.*, 2010. For example, the apparent lead of Antarctic over Greenland temperature variations at orbital timescales could be explained in this way [*Barker et al.*, 2011]. Such a systematic influence is unlikely to be resolved by orbital filtering. In addition, the long timescale associated with large ice sheets also provides a potential explanation for a late response of sea level and certain local northern temperature records [*Imbrie and Imbrie*, 1980; *Alley et al.*, 2002; *Roe*, 2006].

Possible explanations for the global symmetry of glacial cycles generally fall into one of two categories: those that attempt to explain southern variations independently as a direct consequence of southern insolation variability [*Kim et al.*, 1998; *Schulz and Zeebe*, 2006; *Stott et al.*, 2007; *Huybers and Denton*, 2008; *Timmermann et al.*, 2009] and those that rely on an interhemispheric bridge such as the warming effect of North Atlantic Deep Water (NADW) in the Southern Ocean [*Weyl*, 1968; *Imbrie et al.*, 1992] or a global agent such as atmospheric CO_2 concentration [*Alley et al.*, 2002; *Jouzel et al.*, 2007; *Shakun et al.*, 2012]. While there is currently no consensus on this topic, it is instructive to look at individual transitions where highly resolved records and robust chronologies allow detailed investigation.

1.3. The Last Glacial Termination

The last deglaciation, Termination 1 (T1), is the best documented transition between glacial and interglacial conditions. Although the net change across T1 was globally symmetric, millennial-scale changes within either hemisphere were typically asynchronous [*Mix et al.*, 1986; *Sowers and Bender*, 1995; *Denton et al.*, 2006; *Barker et al.*, 2009; *Kaplan et al.*, 2010; *Putnam et al.*, 2010; *Stenni et al.*, 2011; *Shakun et al.*, 2012; *Putnam*, 2013]. For example, during the early phase of T1 (Heinrich Stadial 1, HS1, ~18–14.6 ka) Antarctic temperatures increased while Greenland remained cold (see Figure 5). Warm conditions in the north during the Bølling-Allerød (B-A, 14.6–12.8 ka) were mirrored by decreasing temperatures over Antarctica. The final stage of deglacial warming in the south was accomplished during the northern Younger Dryas (YD) cold interval (12.8–11.5 ka).

Taken together with many others, these observations have led several authors to suggest an implicit role for the bipolar seesaw in the mechanism of deglaciation [*Mix et al.*, 1986; *Broecker and Denton*, 1989; *Clark et al.*, 2004; *Denton et al.*, 2006, 2010; *Barker et al.*, 2009; *Cheng et al.*, 2009; *Wolff et al.*, 2009; *Shakun et al.*, 2012]. Under this scenario, deglacial variations in the AMOC [*McManus et al.*, 2004], possibly triggered by the melting of northern ice sheets in response to increasing northern summer insolation [*Denton et al.*, 2010; *Shakun et al.*, 2012], drove opposing temperature trends in either hemisphere but led ultimately to global warming by the release of atmospheric CO_2 [*Anderson et al.*, 2009; *Barker et al.*, 2009; *Skinner et al.*, 2010] and through positive feedbacks such as the ice albedo effect. Of course the seesaw is probably not the whole story (as hinted at by the fact that earlier analogues of HS1 did not lead to termination [*Barker et al.*, 2009, 2010; *Wolff et al.*, 2009]) and while the relative timing of changes in, e.g., Antarctic temperature and CO_2 [*Parrenin et al.*, 2013] fits with a seesaw scenario, the magnitude of change accomplished during deglaciation suggests that other factors were probably important. Notwithstanding, the observational evidence shows that the last deglaciation was characterized (and perhaps even defined) by interhemispheric asynchronicity on a millennial scale.

1.4. Transition Into a Glacial State

The classic "saw-tooth" view of Late Pleistocene glacial cycles is of a gradual (tens of thousands of years) buildup of continental ice sheets in response to progressively cooler summers in the Northern Hemisphere, followed by their rapid decay during deglaciation [*Broecker and van Donk*, 1970]. But numerous studies have shown that abrupt (hundreds to thousands of years) changes are an intrinsic feature of glacial onset [*Woillard*, 1979; *Keigwin et al.*, 1994; *Schulz et al.*, 1999; *McManus et al.*, 2002; *Cutler et al.*, 2003; *Sima et al.*, 2004; *Ahn and Brook*, 2008; *Barker et al.*, 2011; *Thornalley et al.*, 2013]. The transition from Marine Isotope Stage (MIS) 5a to 4, ~70 ka, is an example of an interglacial-glacial (IG-G) transition where abrupt changes were superimposed on more gradual adjustments. For example, the Antarctic temperature record shows a gradual cooling across MIS 5a/4 that was interrupted by two millennial-scale warming/cooling events associated with D-O oscillations 19 and 20 over Greenland [*Veres et al.*, 2012]. The occurrence of large-amplitude (in terms of Greenland temperature [*Landais et al.*, 2004; *Kindler et al.*, 2013] and the rate of Antarctic temperature change [*Barker et al.*, 2011]) seesaw events during the MIS 5a/4 transition gives rise to the appearance of asynchrony in an analogous way to the changes associated with Termination 1 (Figure 5). However, unlike T1 [*Parrenin et al.*, 2013], variations in atmospheric CO_2 across MIS 5a/4 were not so closely coupled with Antarctic temperature [*Barnola et al.*, 1987] (Figure 6). In fact, the major drop of CO_2 into MIS 4 occurred in parallel with cooling over Greenland at the end of D-O 19 (~70 ka), rather than with Antarctic cooling during D-O 19 [*Ahn and Brook*, 2008; *Bereiter et al.*, 2012]. Here we show that an abrupt shift to more glacial-like conditions ~70 ka is also seen in the SE Atlantic, suggesting a globally synchronous descent into a glacial state.

2. Methods

In this study we extend the records published previously on marine sediment core TNO57-21 (41.1°S, 7.8°E, 4981 m water depth) [*Barker et al.*, 2009, 2010]. TNO57-21 was sampled every 2 cm over its full length (13.8 m). Samples were washed through a 63 μm sieve and dried at 40°C before weighing. Splits of the >150 μm fraction, containing nominally 300 individual planktonic foraminiferal shells, were counted following the taxonomy of *Kennett and Srinivasan* [1983]. Broken shells (less than half a shell) were counted as fragments. Analyses of $\delta^{18}O$ were made on *Globigerina bulloides* (using 20 individual tests where possible) picked from the 250–300 μm fraction. Measurements were performed at Cardiff University stable isotope facility using a Thermofinnigan MAT-252 mass spectrometer for the interval 0–360 cm (long-term external reproducibility better than ±0.08‰) and a Delta Advantage V (long-term external reproducibility ±0.1‰) for the remainder of the core.

2.1. Age Model Construction

Previously [*Barker et al.*, 2009, 2010], we exploited ^{14}C dating of planktonic foraminifer from TNO57-21 and nearby core RC11-83 [*Charles et al.*, 1996] to construct an absolute age model for TNO57-21. From earlier studies [e.g., *Ninnemann et al.*, 1999] we know that TNO57-21 reaches back to about 100 ka, well beyond the range of the ^{14}C method; and we therefore require an alternative solution for extending the age model in this study. Because we wish to compare our surface records directly with ice core data from Greenland and Antarctica, we choose not to use benthic $\delta^{18}O$ tuning (which would lack the precision we require) but instead

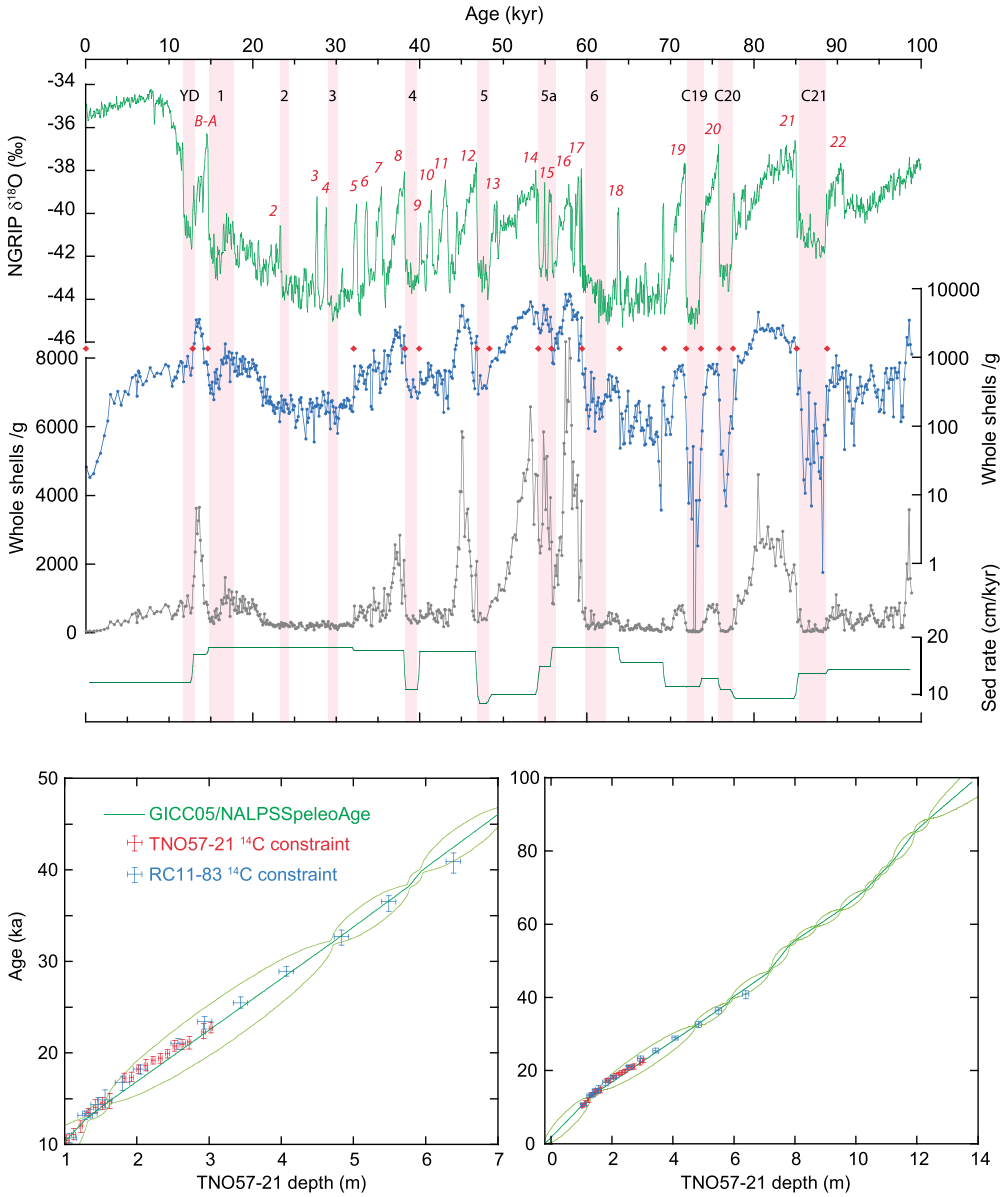

Figure 1. Age model development. (top) The preservation record (whole shells per gram) from TNO57-21 is tuned to the Greenland ice core temperature record [*NGRIP members*, 2004] (red dots are tuning points). Black numbers refer to major cold events over Greenland (including Heinrich Stadials 1–6). Red numbers refer to warm interstadials. (bottom) Calculated uncertainties (2σ) for the tuned age model are shown as green envelopes. The tuned age model generally lies within the 2σ uncertainties of the calibrated ^{14}C dates from TNO57-21 and RC11-83 apart from the interval around HS1. This could be because the reservoir age (held constant at 600 years) is underestimated for this interval.

base our approach on an earlier observation of a relationship between carbonate preservation within TNO57-21 and temperature variations over Greenland [*Barker et al.*, 2010] (Figure 1). Specifically, it was found that well ventilated (with respect to ^{14}C and $[CO_3^{=}]$) bottom waters appeared in the deep South Atlantic during the Bølling-Allerød (B-A, 14.6–12.7 ka). Enhanced preservation (elevated bottom water $[CO_3^{=}]$) was also observed during D-O interstadial 8 (38.2–36.7 ka). Both of these events followed an interval of increased dissolution during HS1 and HS4, respectively. Based on these observations, and a modeling study [*Knorr and Lohmann*, 2007], it was concluded that bottom water ventilation in the region of TNO57-21 is strongly influenced by changes in the nature of deep ocean overturning in the Atlantic, a suggestion previously made based on evidence from benthic foraminiferal $\delta^{13}C$ [*Charles et al.*, 1996; *Ninnemann et al.*, 1999]. In particular,

Table 1. Age Control Points for TNO57-21

Event	Depth in TNO57-21 (cm)	Transition Thickness (cm)	Age (years)[a] GICC05/NALPS	Age Uncertainty (years)[b]
Top	−20	4	0	
Start YD	129.5	6	12,800	430
Start BA	160	8	14,630	360
End D-O5	470.5	4	32,050	400
Start D-O8	576.5	4	38,190	380
End D-O9	594.5	4	39,910	380
Start D-O12	713.5	2	46,830	380
End D-O13	725.5	6	48,310	450
Start D-O14	781.5	2	54,170	340
Start D-O15	804.5	4	55,750	360
Start D-O17	869.5	2	59,410	360
Start D-O18	949.5	2	63,910	400
Start D-O19a	1030.5	4	69,250	360
Start D-O19	1059.5	6	71,875	360
Start C19	1078.5	8	73,625	400
Start D-O20	1106.5	8	75,860	360
Start C20	1123.5	10	77,500	360
Start D-O21	1191.5	8	85,125	360
Start C21	1239.5	14	88,750	360

[a]Ages that are assigned to abrupt transitions in the ice core record and may be adjusted as newer ice core age models become available.
[b]Age uncertainty for input to Bchron [*Parnell et al.*, 2008] is calculated as half of the width of the transition in the ice core record (in time) plus 300 years (see text). Additional uncertainty accounted for in Bchron comes from the width of the transitions within TNO57-21.

it was suggested that recovery of the AMOC, following an interval of weakened circulation, could lead to particularly well ventilated bottom waters in the deep South Atlantic [*Barker et al.*, 2010].

We therefore derive an age model for TNO57-21 by assuming that a similar relationship held for millennial-scale changes over the last 100 kyr (Figure 1). As a tuning target we use the North Greenland Ice Core Project (NGRIP) temperature record as a proxy for AMOC variability. We use the absolute GICC05 timescale back to 60 ka [*Svensson et al.*, 2008]. Beyond this we use a modified version of the absolute timescale developed by *Barker et al.* [2011], which is based on tuning the ice core record to speleothem records (in this case the Northern Alps, NALPS, record of *Boch et al.* [2011]). We select tuning points between TNO57-21 and the NGRIP record (Table 1) based on the record of whole shells per gram in TNO57-21, which was previously highlighted as a reliable indicator of carbonate preservation at this site [*Barker et al.*, 2010]. Uncertainties for individual tie points (with respect to the ice core timescale) are based on the width of the selected transitions in TNO57-21 and the duration of the corresponding transitions in the Greenland record (Table 1). Additional uncertainty stems from the time taken for propagation of signals between Greenland and the deep South Atlantic. Previously, we found that the abrupt signals associated with Greenland warming events within the surface and deep South Atlantic occurred within ~300 years of one another [*Barker et al.*, 2010]. Building on that observation and earlier suggestions of a rapid (decadal) coupling between Greenland (or the surface North Atlantic) and the surface South Atlantic [*Rind et al.*, 2001; *Vellinga and Wood*, 2002; *Schmittner et al.*, 2003; *Timmermann et al.*, 2005; *Barker et al.*, 2009], we suggest that 300 years is a reasonable estimate for signal propagation between Greenland and the deep South Atlantic (we note that this is less than the estimate of 860 ± 220 years attained by paleomagnetic intensity tuning of the same core [*Kissel et al.*, 2008]). We choose to assign an uncertainty of 300 years to our tuning points rather than shift all the tie points toward younger ages since it could be argued that a change to more corrosive waters at our site associated with cooling over Greenland could be accomplished in significantly less than 300 years after the Greenland change.

We apply a Bayesian approach [*Haslett and Parnell*, 2008; *Parnell et al.*, 2008] to estimate age uncertainties between tie points (Figure 1). Estimated age uncertainties can be large (up to 1–3 kyr 2σ) between tie points because of their relative sparsity, implying that we cannot comment on the precise phasing of

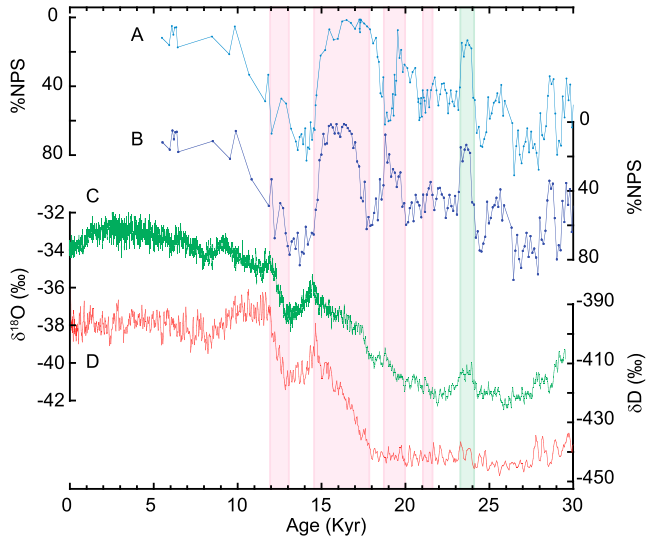

Figure 2. Comparison of age models for TNO57-21 using calibrated ^{14}C ages (A) and our preferred tuning approach (B) with deglacial temperature records from Antarctica (C, D). Green curve is the $\delta^{18}O$ record from WAIS (West Antarctic Ice Sheet) divide [*WAIS Divide Project Members*, 2013]. Red curve is the δD record from EPICA Dome C (EDC) (European Project for Ice Coring in Antarctica Dome C) on the Antarctic ice core chronology (AICC2012) age scale [*Veres et al.*, 2012]. Pink shaded boxes are intervals of significant deglacial warming in the WAIS record according to *WAIS Divide Project Members* [2013]. Green shaded box represents the warming interval preceding D-O 2. "%NPS" refers to the percentage of left coiling *N. pachyderma* to total *N. pachyderma*.

millennial-scale events except those that are close to tie points. However, because our approach is guided by the ^{14}C-based age model used in earlier studies, our tuned age model lies close to the calibrated ^{14}C ages from TNO57-21 and nearby RC11-83 (recalibrated using the CALIB software [*Stuiver and Reimer*, 1993] version 6.1.0 and the MARINE09 calibration curve [*Reimer et al.*, 2009] Figure 1). Our "preservation-tuned" age model is generally within the 95% confidence level of the calibrated ^{14}C dates except for the interval ~17–20 ka, when the revised ages are "too young" with respect to the ^{14}C-derived estimates. While this could reflect a lack of tie points during this interval, we note that the implied onset of surface warming in TNO57-21, previously linked with the start of HS1 [*Barker et al.*, 2009], shifts to ~17.7 ka with the revised timescale as compared to ~18.8 ka when the ^{14}C ages are employed (Figure 2). This younger age is in closer agreement with evidence from Antarctic ice cores that suggests warming initiated ~18 ka [*Parrenin et al.*, 2013] (Figure 2) and would imply that our estimate of surface reservoir age at this site (which was held constant at 600 ± 200 years in our previous calculations) should be increased upward by 6–800 years during this interval. We note a study from a nearby core site [*Skinner et al.*, 2010] that suggested particularly large surface ^{14}C reservoir ages during this same interval, even with respect to the site of TNO57-21.

TNO57-21 is one of many marine cores to reveal a minimum in paleomagnetic intensity associated with the Laschamp event [*Stoner et al.*, 2002]. According to our revised age model, the Laschamp paleomagnetic minimum within TNO57-21 is centered on 42 ka with an estimated 2σ error of −1.4 to +1.8 kyr relative to the GICC05 age model. This should be compared directly with the GICC05 age estimate of the same event (41.2 kyr b1950 ± 1.6 kyr 2σ) [*Svensson et al.*, 2008]. The most recent radioisotopic age estimate for this event is 40.65 ± 0.95 ka [*Singer et al.*, 2009].

Our approach for developing an age model for TNO57-21 is based on the assumption that dissolution within the core is a simple function of mixing between bottom waters with contrasting carbonate chemistry (i.e., northern versus southern-sourced deep waters), but it could be argued that changes in productivity could influence our records either through enhanced carbonate export from the surface ocean or through enhanced pore water dissolution due to organic carbon respiration (previously it was shown that productivity at this site was increased during northern HS events [*Sachs and Anderson*, 2005], which are aligned with intervals of increased dissolution—see *Barker et al.* [2010] for a detailed discussion of these points). On the other hand, our approach follows previous studies that first highlighted a link between Greenland climate variability (if viewed as a surrogate for AMOC variability) and deep water mass mixing in the Cape Basin [*Charles and Fairbanks*, 1992; *Charles et al.*, 1996; *Ninnemann et al.*, 1999; *Piotrowski et al.*, 2005]. We can therefore provide a test of our age model by assessing its implications for other deep water proxies measured on proximal cores recovered from the deep Cape Basin (see supporting information). The close correspondence between carbonate preservation, benthic $\delta^{13}C$ and sedimentary Nd isotopes within TNO57-21, and the similarity in records of benthic $\delta^{13}C$ in the Cape Basin cores versus Iberian Margin core MD95-2042 [*Shackleton et al.*, 2000] (Figure S1 in the supporting information) strongly supports the contention that changes in deep ocean circulation dominate the variability in these diverse proxy records.

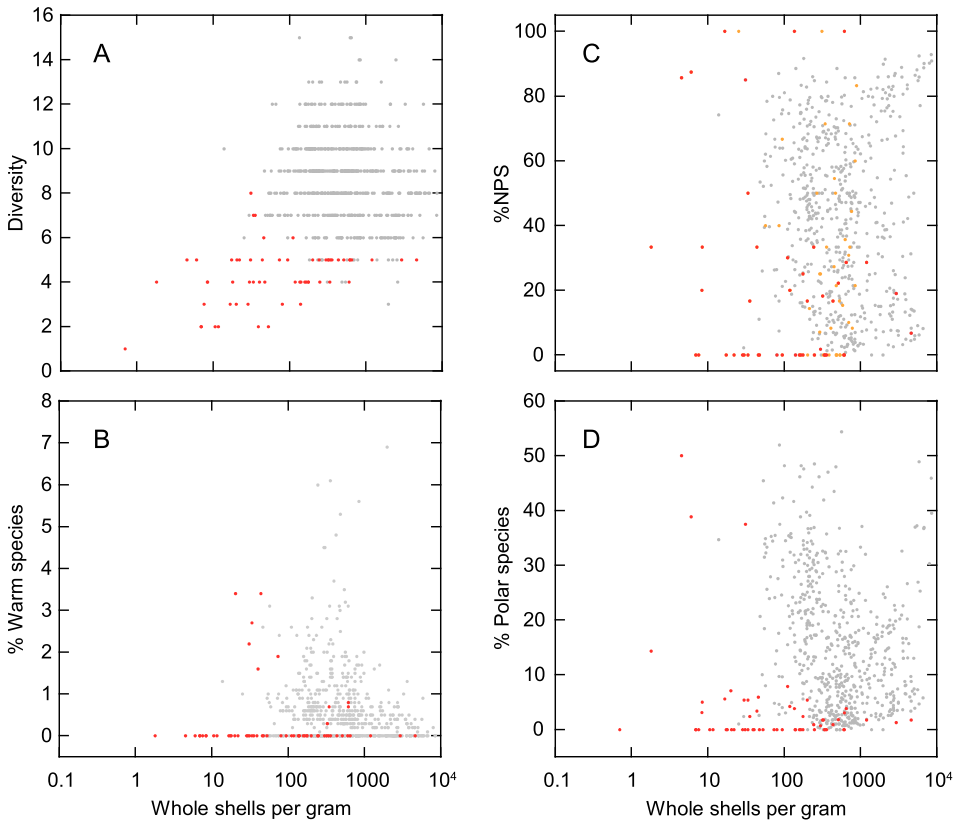

Figure 3. Samples thought to be compromised by dissolution are rejected (red symbols) based on the following criteria: Species diversity <6 and %*G. inflata* > %*G. bulloides* and/or samples with <50 whole shells counted. For %NPS (/total *N. pachyderma*) we also reject samples with total *N. pachyderma* counted <15 (orange symbols).

Differences between the records may reflect deficiencies in the individual proxies or perhaps the lower resolution of some records. While it could be argued that disagreement between the records from TNO57-21 should be taken into account within our age model uncertainties, we suggest that the abrupt nature of the preservation changes we record reflect the superior ability of this record to reflect the abrupt circulation changes in which we are interested. Furthermore, we believe that the record of whole shells per gram is superior to other dissolution indicators (such as $\%CaCO_3$; Figure S1) again due to the abrupt nature of the changes we observe, which suggest minimal smearing of the signal through sedimentary processes.

2.2. Effects of Dissolution on Planktonic Foraminiferal Assemblages

At a site as deep as TNO57-21 (~5 km water depth) even a core with such high sedimentation rates as TNO57-21 will have experienced significant carbonate dissolution. This is apparent from the occasionally low $\%CaCO_3$ (supporting information Figure S1) and the fragmentation of foraminiferal tests observed in the core [*Barker et al.*, 2010]. It is well known that dissolution can affect planktonic foraminiferal assemblages by the preferential breakup of species with more fragile shells [*Ruddiman and Heezen*, 1967; *Berger*, 1970; *Le and Thunell*, 1996]. In a separate paper, M. J. Vautravers et al. (manuscript in preparation, 2014) discuss the potential influence of dissolution on the faunal assemblages derived in this study. They show that samples with a low species diversity (<6) are generally associated with the most intense dissolution (Figure 3). On the other hand, low species diversity does not necessarily mean that the sample is highly dissolved, for example, a polar assemblage will have only a few species present whatever the state of preservation. Vautravers et al. (manuscript in preparation, 2014) also note that the majority of those samples with diversity <6 are dominated by the solution resistant species, *Globorotalia inflata* (14/22 on *Berger's* [1970] ranking of susceptibility to dissolution where 1 is most susceptible), while those with greater diversity tend to be dominated by the less robust species, *G. bulloides* (ranked 8/22). They suggest that if these two criteria (diversity <6 and %*G. inflata* > %*G. bulloides*) are met, then the assemblage is most likely compromised by

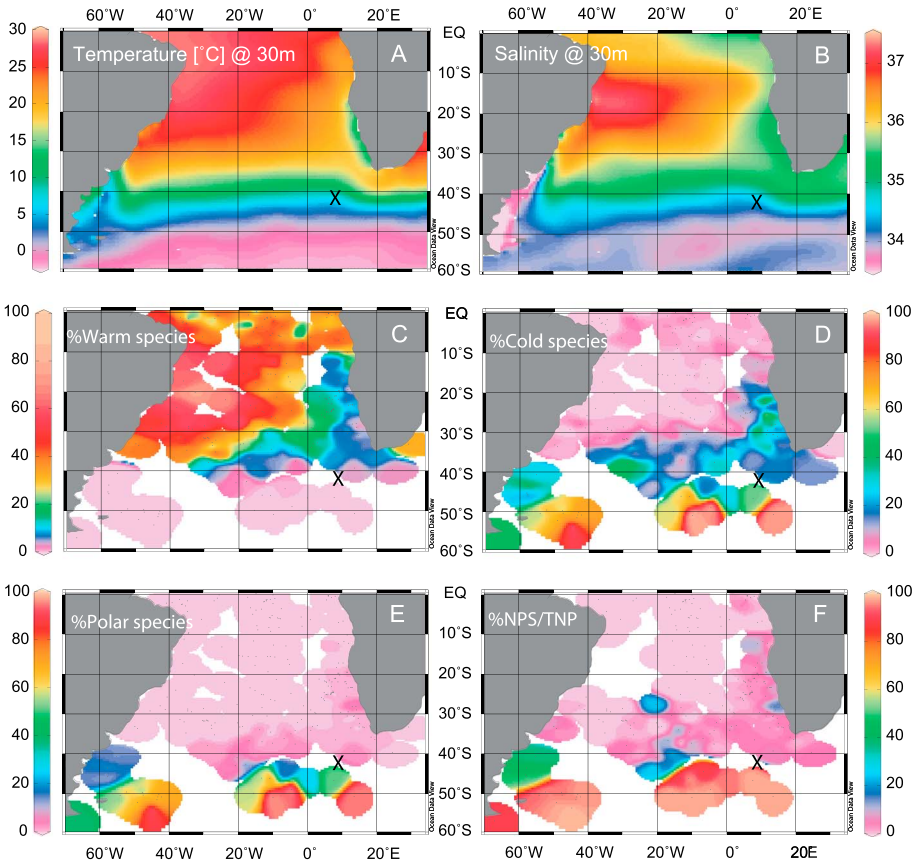

Figure 4. (a, b) Modern mean annual temperature [*Locarnini et al.*, 2010] and salinity [*Antonov et al.*, 2010] at 30 m depth for the SASO region. (c–f) Coretop data from the Multi Proxy Approach for the Reconstruction of the Glacial Ocean Surface (MARGO) database [*Kucera et al.*, 2005] showing the sensitivity of the specific faunal groups used here to conditions in the region. Site of TNO57-21 is marked with an X. Note that %NPS (/total *N. pachyderma*) shifts from zero to 100% at the location of our site. Plots were created using the Ocean Data View (ODV) software [*Schlitzer*, 2014].

dissolution and should not be used to make inferences about surface temperature. Here we follow these criteria and also reject samples with <50 whole shells counted. In all, we reject 61 out of 658 samples counted (Figure 3). For the plots of %NPS (percentage of *Neogloboquadrina pachyderma* (sin) out of total *N. pachyderma*), we also exclude those samples with total *N. pachyderma* counted <15 (total of 94 samples rejected).

Due to the potential for dissolution to bias faunal temperature estimates we use groups of index species in an attempt to further minimize the potential influence of dissolution (Figures 4–6). For example, the polar group consists of *Turborotalita quinqueloba* (ranked 9/22 by *Berger* [1970]) and *N. pachyderma* (sin) (ranked 17/22) while the warm group contains *Globigerinoides ruber* (1/22), *Orbulina universa* (2/22), *Globorotalia hirsuta* (12/22), and *Globorotalia truncatulinoides* (dex) (13/22). Similar trends in the relative proportions of species within these groupings, even those with very different susceptibilities to dissolution (see supporting information), give us confidence that dissolution is not the primary signal in our records and that we are able to observe changes in the original assemblage (i.e., we are able to discuss changes in sea surface conditions).

3. Results and Discussion

3.1. Millennial-Scale Changes: the Bipolar Seesaw

A prominent feature of the planktonic assemblage records reported here is the abrupt nature of some of the changes we observe (Figure 5). These are particularly striking in the record of %NPS. With some notable exceptions [*Kaiser et al.*, 2005; *Lamy et al.*, 2007] the majority of high-resolution temperature records from the Southern Hemisphere display rather gradual changes, reminiscent of the Antarctic temperature record

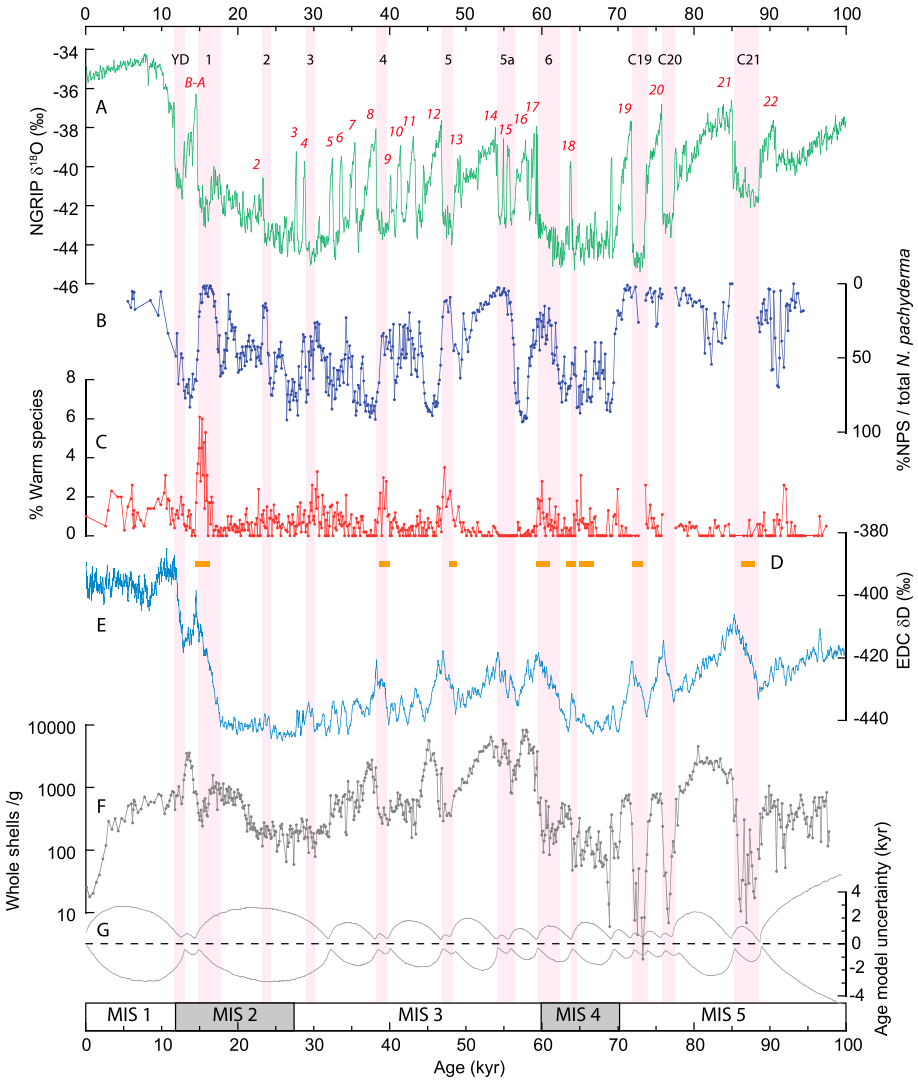

Figure 5. Records of %NPS/total *N. pachyderma* (B) and warm species (C) from TNO57-21 compared with Greenland [*NGRIP_members*, 2004] (A) and Antarctic [*Jouzel et al.*, 2007] (E) ice core temperature records and the speleothem growth interval record from Brazil [*Wang et al.*, 2004] (D). The preservation record from TNO57-21 (F) is also shown to allow assessment of the tuning procedure. Estimated uncertainties for the tuned age model (calculated by Bchron [*Parnell et al.*, 2008]) are shown in (G). The NGRIP record is on the GICC05/NALPS age model described in the text. The Antarctic record has been placed on the same timescale following the procedure described by *Barker et al.* [2011].

[*Pahnke and Sachs*, 2006]. In contrast, we observe clear aspects of similarity (albeit in antiphase) between our SE Atlantic records and the abrupt temperature variations recorded in Greenland over the last 65 kyr. Large and abrupt shifts from low to high %NPS (indicating cooling at our site) tend to parallel strong warming events in Greenland, typically those following Heinrich Stadial (HS) events. Most of the northern HS events are aligned with an increase in warm species at our site and a decrease in %NPS. Previously, we called on a latitudinal shift (of perhaps a few degrees) in the position of the thermal Subtropical Front (STF) to explain the abrupt assemblage changes we observed during T1. Given the large latitudinal gradients in sea surface temperature associated with the frontal zones in this region [*Deacon*, 1982; *Orsi et al.*, 1995] (Figure 4a), we feel that this is more reasonable than calling on large temperature changes of specific water masses, which would also be contrary to modeling studies [*Vellinga and Wood*, 2002; *Timmermann et al.*, 2007]. The modern distribution of %NPS in the SASO region [*Margo Project Members*, 2009] (Figure 4) demonstrates how sensitive our site is to minor shifts in the frontal positions. We suggest that, in general, cold northern HS events were paralleled by a southward shift of the thermal STF in the SE Atlantic, followed by a northward

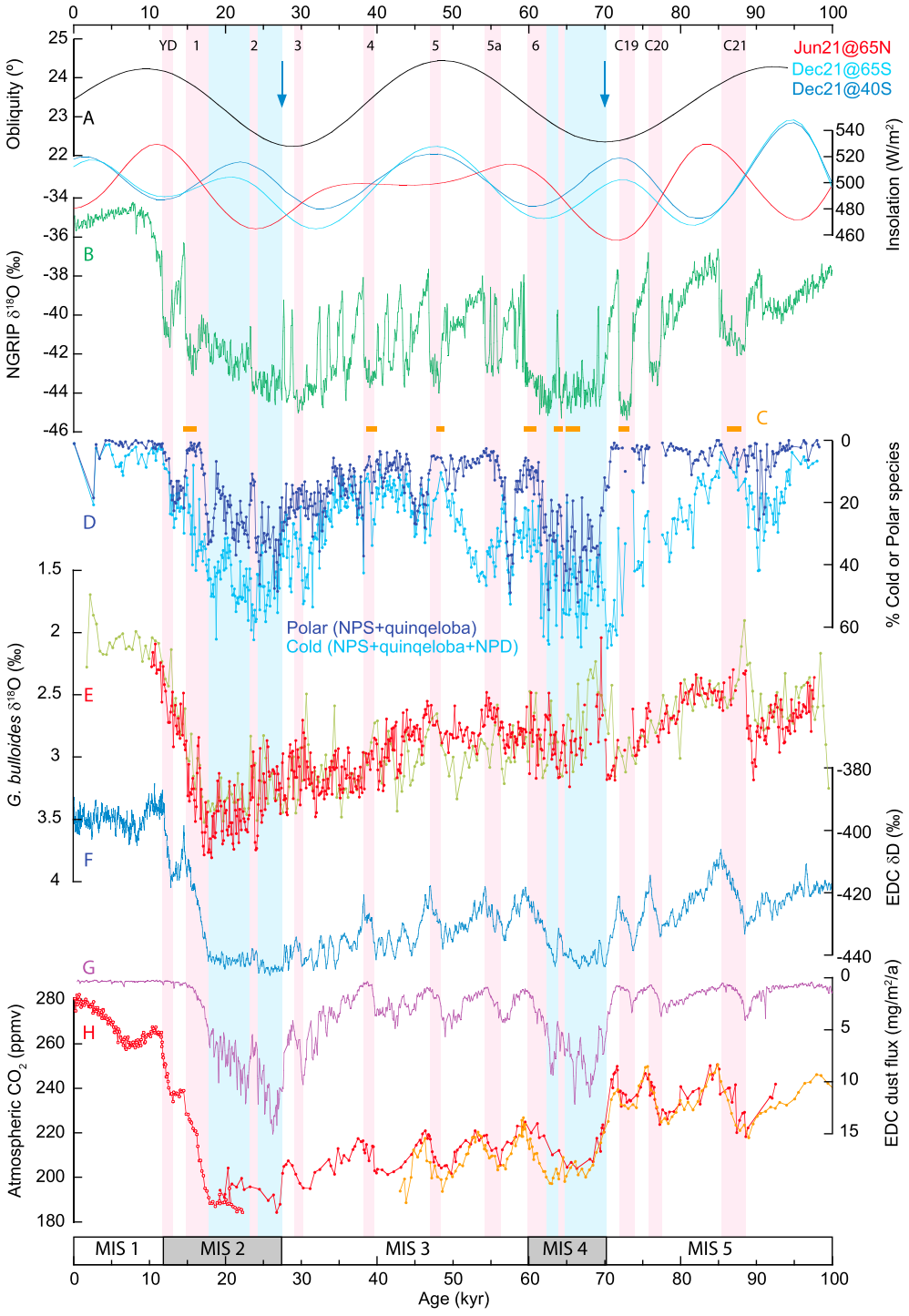

Figure 6. The record of cold foraminiferal species from TNO57-21 (D) reveals gradual cooling across MIS 5/4 while the polar species record suggests an abrupt cooling ~70 ka. (E) δ^{18}O records from *G. bulloides* (red is this study, green is from *Mortyn et al.* [2002]) generally show shifts toward lighter values during Antarctic warming events but a significant depletion is associated with cold conditions during early MIS 4. Also shown are records of obliquity [*Berger and Loutre*, 1991] and insolation [*Laskar et al.*, 2004] (A), Greenland δ^{18}O [*NGRIP_members*, 2004] (B), Brazilian speleothem growth [*Wang et al.*, 2004] (C), Antarctic δD [*Jouzel et al.*, 2007] (F), Antarctic dustiness [*Lambert et al.*, 2012] (G), and atmospheric CO_2 [*Monnin et al.*, 2001; *Ahn and Brook*, 2008; *Bereiter et al.*, 2012] (H). Blue arrows point to similar changes occurring ~70 and ~27 ka. All ice core records are on the GICC05/NALPS timescale.

shift with the subsequent return to interstadial conditions. A notable exception is HS5a and D-O14. Conditions at our site during HS5a were not conducive to warm species, although we do observe a decrease in %NPS at the start of this period. Furthermore, the start of D-O14 was not marked by a major increase in %NPS at our site, but by a rather modest increase in total cold species present (Figure 6), suggesting that this "AMOC recovery" was not as pronounced as other events.

We do not see clear evidence for systematic variations associated with non-H oscillations. While this could in part reflect the difficulty in resolving short events within a marine core, sedimentation rates in TNO57-21 (typically $>$15 cm/kyr during the intervals of concern) should be sufficient to resolve features associated with even fairly short (1–2 kyr) events, regardless of the fact that our age model is too imprecise to discuss their relative timing. We are therefore confident that, at least in terms of surface temperature, northern HS events and their subsequent interstadials were associated with more significant perturbations at our site than non-Heinrich oscillations. Many previous studies have highlighted the anomalous conditions associated with HS events as compared with non-H stadials [*Bond et al.*, 1993; *Cacho et al.*, 1999; *Wang et al.*, 2004]. The fact that we also tend to see larger perturbations associated with the interstadials following HS events further illustrates their anomaly.

Following our previous work [*Barker et al.*, 2009], we suggest that the variations we observe during the last 65 kyr represent the southern end of the "instantaneous" bipolar seesaw, as predicted by the conceptual model of *Stocker and Johnsen* [2003]. We interpret our records to reflect latitudinal shifts in the northernmost thermal frontal zone of the Antarctic Circumpolar Current (ACC), corresponding to abrupt temperature changes over Greenland. Model experiments have shown that atmospheric phenomena, such as the Intertropical Convergence Zone and the southern westerly wind belt can shift southward in response to a cooling across the North Atlantic [*Vellinga and Wood*, 2002; *Chiang et al.*, 2003; *Chiang and Bitz*, 2005; *Timmermann et al.*, 2007]. These predictions are supported by paleostudies in the low latitude Atlantic region [*Peterson et al.*, 2000; *Wang et al.*, 2004] and, we argue, by our results from the SE Atlantic. Furthermore, our evidence suggests not only that HS events were anomalous with respect to other cold intervals but also that the interstadials directly following HS events were correspondingly anomalous. Model experiments also suggest that, following an interval of weakened circulation, the AMOC can overshoot with respect to its equilibrium state on recovery [*Ganopolski and Rahmstorf*, 2001; *Knorr and Lohmann*, 2007; *Ganopolski and Roche*, 2009; *Liu et al.*, 2009]. Previously, [*Barker et al.*, 2010] we argued that our observation of particularly well ventilated deep waters at the site of TNO57-21 during the B-A and D-O 8 provided evidence of AMOC overshoots following HS1 and HS4, respectively. Here we suggest that our planktonic assemblage results also support the idea that the climate system experienced a pronounced rebound following the extreme perturbations associated with Heinrich Stadial events.

3.2. Marine Isotope Stage 4

A major feature of our new records from TNO57-21 is an abrupt cooling at the onset of MIS 4 (~70 ka) as implied by a large increase in the abundance of polar species (Figure 6). Significantly, this occurred approximately in parallel with cooling across Greenland, i.e., this was not an expression of the bipolar seesaw, but an interhemispheric cooling that was approximately synchronous with the glacial lowering of CO_2 (Figure 6). The abrupt cooling we observe at ~70 ka may be contrasted with the more gradual cooling recorded over Antarctica across MIS 5a/4. Severe carbonate dissolution in TNO57-21 during cold stadial events C19, 20, and 21 means that we have had to reject several samples as unreliable during these intervals, but we do observe a more gradual increase in cold species (*N. pachyderma* (s) + *T. quinqueloba* + *N. pachyderma* (d)) that parallels the Antarctic trend across this interval. The cold species record also shows the superposition of what appears to be seesaw-like behavior associated with D-O 19–21 although this is not so clear (Figures 6 and 7). On the other hand, several studies have demonstrated a clear seesaw response in atmospheric and deep ocean conditions in the Atlantic sector across the MIS 5/4 transition [*Keigwin et al.*, 1994; *Peterson et al.*, 2000; *Wang et al.*, 2001; *Wang et al.*, 2004; *Weldeab et al.*, 2007; *Thornalley et al.*, 2013] (Figures 5 and 6). In this respect we may have expected to observe corresponding behavior in our records. According to the seesaw model we might also have expected to see warming at our site ~70 ka, associated with the demise of northern warmth at the end of D-O 19 and while there is a decrease in cold species at this time, this is paralleled by the increase in polar species (a subset of the cold group) and %NPS, suggesting an overall shift to colder conditions.

The record of polar species from TNO57-21 suggests that conditions in the SE Atlantic during early MIS 4 may have been colder than during MIS 2 (Figure 6). This observation of severe glacial conditions during MIS 4 is in

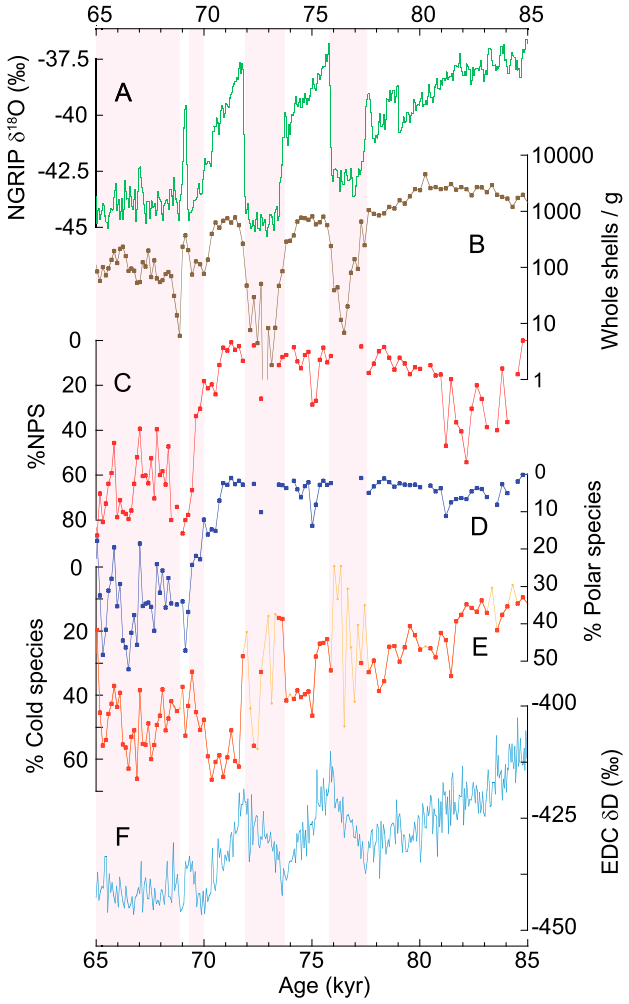

Figure 7. The MIS 5/4 transition in TNO57-21. (A) Greenland $\delta^{18}O$ [*NGRIP members*, 2004], (B) Whole shells per gram, (C) %NPS/total *N. pachyderma*, (D) Polar species, (E) Cold species, (F) Antarctic δD [*Jouzel et al.*, 2007]. Faint data points and conjoining lines in (E) are samples that are highly dissolved and omitted from the main discussion.

line with several other studies. For example, an alkenone-based sea surface temperature reconstruction from a sediment core taken offshore Namibia (23.4°S, 11.7°E), directly downstream from our core site, also shows an abrupt onset of glacial conditions at MIS 4 that were more extreme than either MIS 2 or 6 [*Kirst et al.*, 1999]. Another high-resolution alkenone-SST record from the SE Pacific also shows coldest conditions during MIS 4 [*Kaiser et al.*, 2005]. Mountain glaciers in New Zealand (J. M. Schaefer et al., The Southern Glacial Maximum 65,000 years ago and its Unfinished Termination, submitted to *Quaternary Science Reviews*, 2014) and in parts of Chile [*Denton et al.*, 1999] extended further down-valley during MIS 4 than MIS 2, suggesting that MIS 4 could have been the "Last Glacial Maximum (LGM) of the south." *Kaiser et al.* [2005] interpreted their temperature record from the SE Pacific to reflect latitudinal shifts in the ACC and midlatitude westerlies. They suggested that the coupled ACC-subtropical gyre system may have experienced a wholesale equatorward shift of 5–6° during MIS 4 (compared with 4–5° during the LGM). This interpretation would fit with our observation of particularly cold conditions in the SE Atlantic during the same period. However, our $\delta^{18}O$ results suggest that the situation was more complex.

The $\delta^{18}O$ record from *G. bulloides* (Figure 6) shows a large (0.7–1‰) shift to lighter values ~70 ka, in parallel with the cooling inferred from %NPS and the polar species group. This is in contrast to other intervals where lighter values of $\delta^{18}O$ in *G. bulloides* are associated with episodes of warming at our site (when lighter $\delta^{18}O$ presumably reflected warming associated with the bipolar seesaw [*Charles et al.*, 1996; *Ninnemann et al.*, 1999; *Barker et al.*, 2009]). Severe carbonate dissolution throughout this interval means that we were unable to derive a reliable record of foraminiferal Mg/Ca that would enable us to disentangle the relative influences of temperature and $\delta^{18}O_{sw}$ within the $\delta^{18}O$ record. However, if the shift in $\delta^{18}O$ at 70 ka were due solely to a temperature change, this would require a warming of approximately 3–4°C [*Shackleton*, 1974; *Bemis et al.*, 1998]. If the change were due solely to variations in $\delta^{18}O_{sw}$, this would equate to a salinity shift of approximately -1.5 to -2 practical salinity unit (psu; if the relationship between $\delta^{18}O_{sw}$ and salinity was the same as modern) [*Charles and Fairbanks*, 1990; *LeGrande and Schmidt*, 2006]. Given the steep latitudinal gradient in salinity across the STF (Figure 4b), it would be tempting to interpret the decrease in *G. bulloides* $\delta^{18}O$ at 70 ka to reflect a northward shift of the frontal system, bringing fresher water over the site of TNO57-21. However, the strong temperature effect on foraminiferal $\delta^{18}O$ means that we should expect the opposite effect if we were to shift the modern frontal system northward (Figure 8a). A freshening of the surface Southern Ocean could explain some of the change we observe, but this would have had to have been extreme (perhaps 3–4 psu) to completely overcome the colder temperatures. Furthermore, the same shift in $\delta^{18}O$ is not seen for the deeper dwelling species *G. truncatulinoides* at the same site [*Mortyn et al.*, 2002].

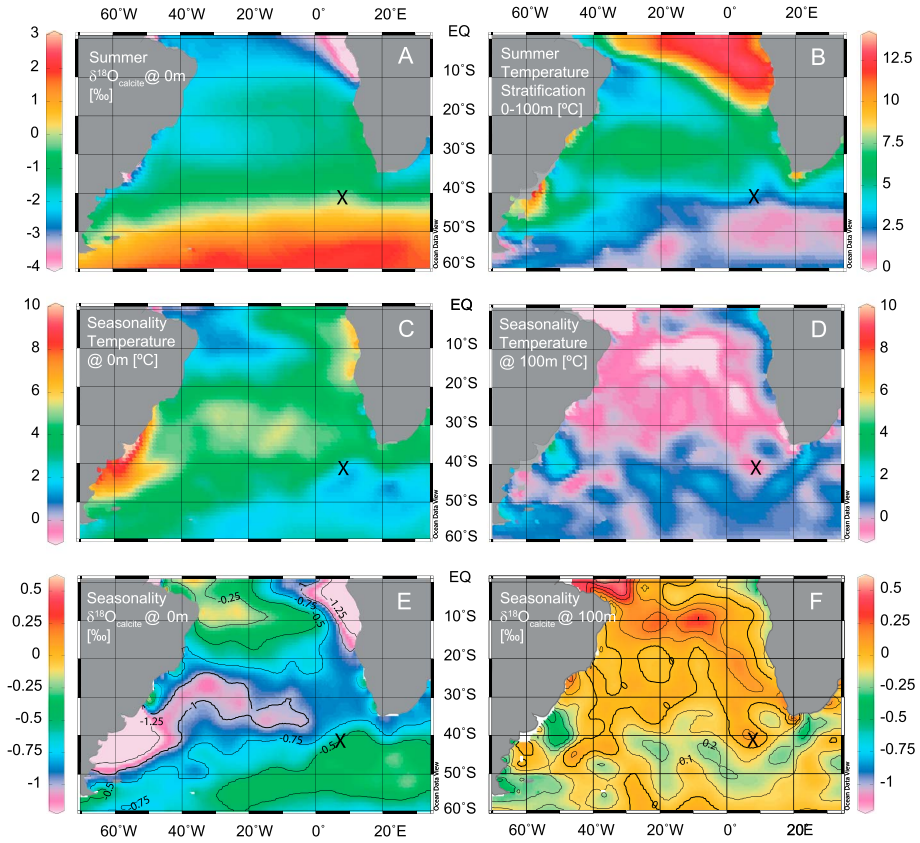

Figure 8. (a) Predicted equilibrium calcite $\delta^{18}O$ for austral summer (January-February-March) reveals the dominant control of temperature (cf. Figure 5). $\delta^{18}O_{calcite}$ was calculated using the temperature equation of *Bemis et al.* [1998] ($T = 13.2 - 4.9*(\delta^{18}O_{calcite} = \delta^{18}O_{sw})$), where $\delta^{18}O_{sw}$ was calculated from salinity ($\delta^{18}O_{sw} = 0.5*S - 17.25‰$ [*Charles and Fairbanks*, 1990; *LeGrande and Schmidt*, 2006]) and converted from standard mean ocean water to Peedee belemnite by a correction factor of −0.27‰ [*Hut*, 1987] (b) Summer stratification of the upper water column occurs north of the STF. Strong seasonality in (c) sea surface temperature results in a wide seasonal range of (e) predicted calcite $\delta^{18}O$ compared to conditions at (d, f) 100 m. Contours in Figure 8e are every 0.25‰ and in Figure 8f are every 0.1‰. Plots created by ODV [*Schlitzer*, 2014].

In fact, the offset in $\delta^{18}O$ between *G. bulloides* and *G. truncatulinoides* is greater during MIS 4 than during the Holocene (or any other time over the last 100 ka) [*Mortyn et al.*, 2002]. Given that upper water column stratification is significantly reduced south of the modern STF (Figure 8b), the shift toward lighter $\delta^{18}O$ of *G. bulloides* and the increased offset between surface and deep dwelling species could lead to the conclusion that the STF actually shifted south of our site during MIS 4.

To reconcile these observations, we call on enhanced seasonality of sea surface temperatures and stronger latitudinal temperature gradients within the South Atlantic/Southern Ocean region during MIS 4 with respect to modern conditions. We posit that the combination of colder mean conditions, as suggested by our faunal results and previous studies [*Kirst et al.*, 1999], together with a maximum in midlatitude Southern Hemisphere summer insolation (Figure 6), resulted in a stronger seasonal contrast in surface waters of the SASO region. Low obliquity at this time would also have meant enhanced latitudinal temperature gradients in the region of the STF (Figure 6). This combination could have resulted in more seasonal to interannual variability in the latitudinal position of the thermal STF, resulting in the admixture of species from a wider range of conditions than observed in the modern assemblage at our site even if the mean position of the front was shifted northward. The large annual range in sea surface temperature within the modern SASO corresponds to a range in predicted $\delta^{18}O_{calcite}$ of 0.5–1‰ (Figure 8e). Given the tendency for foraminifera to shift their season of growth to warmer months when mean annual conditions are colder [*Fraile et al.*, 2009], we suggest that the lighter $\delta^{18}O$ values observed for *G. bulloides* may in part be explained by a relatively warmer season of growth and sporadic migration of the thermal STF, bringing warmer waters over our site.

The lack of response in *G. truncatulinoides* [*Mortyn et al.*, 2002] could reflect the small seasonal temperature range at the deeper depths more typical of this species (Figure 8f).

The modern surface Southern Ocean is relatively fresh due to continental runoff and an excess of precipitation over evaporation [*Wüst et al.*, 1954; *Gordon*, 1971], countered in part by the upwelling of warm and salty Circumpolar Deep Water (CDW) [*Gordon*, 1971]. *Toggweiler et al.* [2006] argued that a northward shift in the westerly wind belt could reduce the upwelling of CDW, leading to a freshening of surface waters. Enhanced freshening could also result from increased seasonal sea ice formation [*Gordon*, 1971]. These factors could also have contributed to the lighter δ^{18}O values we observe during MIS 4.

3.3. Descent Into an Ice Age

Our new records demonstrate a sense of duality in the transition from MIS 5 to 4. The gradual increase in cold species resembles the cooling trend displayed by the Antarctic ice core record (even though the seesaw response is not so clear in our records). Contrasted with this is the abrupt descent into glacial stage 4, around 70 ka, as evidenced by our record of polar species. This duality is also observed elsewhere. For example, benthic δ^{18}O records suggest that decreasing sea level and/or deep ocean temperature mirrored the decrease in Antarctic temperature [*Waelbroeck et al.*, 2002; *Siddall et al.*, 2003] whereas atmospheric CO_2 and Antarctic dustiness experienced a more rapid transition into MIS 4 also ~70 ka (Figure 6). We suggest that a combination of orbital configuration and ocean/atmosphere circulation changes could have been responsible for the various responses observed.

Orbital-timescale cooling over Greenland across MIS 5/4 was probably driven by the reduction in northern summer insolation (Figure 6). The concurrent cooling over Antarctica and the Southern Ocean could in part have been the result of longer winters [*Huybers and Denton*, 2008] but we note that all of the cooling throughout this interval occurred during warm intervals in Greenland (i.e., intervals of strong northward meridional heat transport associated with a "positive phase" of the bipolar seesaw). However, we suggest that it was not just northward heat piracy [*Crowley*, 1992] that drove Antarctic cooling across MIS 5/4, but the added effect of colder North Atlantic Deep Water (NADW) being formed, a result of colder northern summers (for example, through the connection between summer mixed layer temperature and the initiation of Arctic sea ice formation during the subsequent fall and winter [*Stroeve et al.*, 2012]). When the AMOC was strong (during interstadials 19–21), northward heat piracy cooled the surface to intermediate depth Southern Ocean along the ideas of *Crowley* [1992]. At the same time, the influence of colder NADW led to a cooling of CDW and thus amplified the cooling of Southern Ocean waters. This interaction provides a possible explanation for orbital-timescale cooling across MIS 5/4 but the abrupt change we observe at ~70 ka suggests that a threshold was crossed at this time, possibly as a consequence of accelerated Southern Ocean cooling during D-O interstadial 19.

Recent work in the North Atlantic has illustrated the nature of circulation changes (specifically involving the Western Boundary Undercurrent, WBUC) throughout MIS 5/4 [*Thornalley et al.*, 2013]. The study suggested that the WBUC effectively shoaled during cold events C19 and C20 in agreement with nutrient proxy evidence that points to the enhanced presence of southern-sourced deep waters within the Atlantic during these cold events [*Keigwin and Jones*, 1994; *Shackleton et al.*, 2000] (supporting information Figure S1). More significantly, the results of *Thornalley et al.* [2013] suggest that the WBUC shoaled further during MIS 4 than during C19 and 20, implying that a distinct change in the vertical structure of the Atlantic Ocean occurred at approximately the same time as atmospheric CO_2 dropped and when we observe the transition to extreme glacial conditions in the SE Atlantic. Pronounced shoaling of the AMOC during MIS 4, as also suggested by strong δ^{13}C depletion and carbonate dissolution at relatively shallow water depths in the midlatitude Atlantic [*Curry and Lohmann*, 1986; *Curry*, 1996], would have provided increased capacity for deep ocean carbon storage and could in part explain the large drop in atmospheric CO_2 at this time. Raising the boundary between cold and salty Antarctica Bottom Water and less dense NADW during glacial times would also have alleviated the effects of vertical mixing due to rough topography [*Lund et al.*, 2011; *Adkins*, 2013], thus providing a more effective carbon trap.

Model results suggest that a critical factor in generating a state of ocean circulation with pronounced vertical stratification (in this case during the LGM but MIS 4 could provide a suitable analogy) is the preexistence of a stratified deep ocean, possibly as a result of enhanced sea ice formation and brine rejection in the Southern

Ocean as a consequence of low obliquity [*Zhang et al.*, 2013] (we note that changes ~27 ka are somewhat analogous to those ~70 ka and both are times of low obliquity; Figure 6). Such conditions may have been approached as obliquity decreased from ~90 to 70 ka, but apparently the system was not primed sufficiently for the circulation shifts associated with cold events C19 and C20 to trigger the switch to a sufficiently stratified deep ocean. We hypothesize that accelerated cooling across the Southern Ocean during D-O 19 provided the final push necessary for the switch to deep ocean stratification and the descent into full glacial conditions ~70 ka. At this time, northward shifted winds [*Toggweiler et al.*, 2006] could have provided a positive feedback by effectively dampening overturning in the Southern Ocean, producing a freshwater lid and cooling the entire Subantarctic region (as supported by our observations). Increased sea ice formation around Antarctica, aided by the colder conditions and reduced melting of Antarctic ice shelves [*Miller et al.*, 2012; *Adkins*, 2013], would have produced the dense bottom waters required to provide stable accommodation space for the accumulation of carbon, which may also have been aided by increased efficiency of the biological pump in response to enhanced glacial dustiness [*Martinez-Garcia et al.*, 2011]. Once these conditions were achieved the alleviating effects of subsequent abrupt circulation changes could not penetrate the quasi-stability of the stratified glacial ocean [*Barker et al.*, 2010], and climate remained cold until HS6 and the transition into MIS 3.

4. Conclusions

Our new records from TNO57-21 describe the nature of millennial-scale variability in the SE Atlantic over the last 100 kyr. Similar to the last deglaciation, millennial-scale variability throughout MIS 3 and 2 was characterized by interhemispheric asynchrony (the bipolar seesaw); and while similar variability adorned the transition from MIS 5 to 4, the abrupt descent into glacial conditions, ~70 ka, (perhaps the most significant transition of the last 100 kyr in our records) was globally synchronous. We suggest that a combination of changing orbital configuration (decreasing northern summer insolation cooling NADW combined with decreasing obliquity in promoting sea ice formation in the Southern Ocean) and the compounding effects of abrupt changes in ocean/atmosphere circulation patterns (the bipolar seesaw) drove the system across a threshold whereby ocean circulation could enter its glacial mode. The consequent lowering of atmospheric CO_2 and reduced overturning of the Southern Ocean sealed the fate of Earth's climate until the end of MIS 4.

Acknowledgments

Planktonic faunal counts were performed by M. Vautravers as part of NERC (UK) project NE/G004021/1. We thank H. Medley for assistance in the laboratory, A. Parnell for advice on the use of Bchron, and S. Heckendorff for advice on ODV. We thank G. Knorr and D. Thornalley for helpful comments. Sample material used in this project was provided by the Lamont-Doherty Earth Observatory Deep-Sea Sample Repository. We thank Rusty Lotty and George Lozefski for their help with sampling. Support for the collection and curating facilities of the core collection is provided by the National Science Foundation through grant OCE00-02380 and the Office of Naval Research through grant N00014-02-1-0073. The work was supported by the UK Natural Environment Research Council (grants NE/F002734/1 and NE/G004021/1) and through a Philip Leverhulme prize to S.B. We thank the Editor (C. Charles), A. Piotrowski and an anonymous reviewer for their thoughtful comments. All data sets presented in this paper are tabulated within the supporting information.

References

Adkins, J. F. (2013), The role of deep ocean circulation in setting glacial climates, *Paleoceanography*, *28*, 539–561, doi:10.1002/palo.20046.

Ahn, J., and E. J. Brook (2008), Atmospheric CO_2 and climate on millennial time scales during the last glacial period, *Science*, *322*(5898), 83–85.

Alley, R. B., E. J. Brook, and S. Anandakrishnan (2002), A northern lead in the orbital band: North–south phasing of Ice-Age events, *Quat. Sci. Rev.*, *21*(1–3), 431–441.

Anderson, R. F., S. Ali, L. I. Bradtmiller, S. H. H. Nielsen, M. Q. Fleisher, B. E. Anderson, and L. H. Burckle (2009), Wind-driven upwelling in the Southern Ocean and the deglacial rise in atmospheric CO_2, *Science*, *323*(5920), 1443–1448.

Antonov, J. I., D. Seidov, T. P. Boyer, R. A. Locarnini, A. V. Mishonov, H. E. Garcia, O. K. Baranova, M. M. Zweng, and D. R. Johnson (2010), in *World Ocean Atlas 2009, Volume 2: Salinity*, NOAA Atlas NESDIS 69, edited by S. Levitus, 184 pp., U.S. Government Printing Office, Washington, D. C.

Barker, S., P. Diz, M. J. Vautravers, J. Pike, G. Knorr, I. R. Hall, and W. S. Broecker (2009), Interhemispheric Atlantic seesaw response during the last deglaciation, *Nature*, *457*(7233), 1097–1102.

Barker, S., G. Knorr, M. Vautravers, P. Diz, and L. C. Skinner (2010), Extreme deepening of the Atlantic overturning circulation during deglaciation, *Nat. Geosci.*, *3*, 567–571, doi:10.1038/ngeo921.

Barker, S., G. Knorr, R. L. Edwards, F. Parrenin, A. E. Putnam, L. C. Skinner, E. Wolff, and M. Ziegler (2011), 800,000 years of abrupt climate variability, *Science*, *334*(6054), 347–351.

Barnola, J. M., D. Raynaud, Y. S. Korotkevich, and C. Lorius (1987), Vostok ice core provides 160,000-year record of atmospheric CO_2, *Nature*, *329*(6138), 408–414.

Bemis, B. E., H. J. Spero, J. Bijma, and D. W. Lea (1998), Reevaluation of the oxygen isotopic composition of planktonic foraminifera: Experimental results and revised paleotemperature equations, *Paleoceanography*, *13*(2), 150–160, doi:10.1029/98PA00070.

Bereiter, B., D. Luthi, M. Siegrist, S. Schupbach, T. F. Stocker, and H. Fischer (2012), Mode change of millennial CO2 variability during the last glacial cycle associated with a bipolar marine carbon seesaw, *Proc. Natl. Acad. Sci. U.S.A.*, *109*(25), 9755–9760.

Berger, A., and M. F. Loutre (1991), Insolation values for the climate of the last 10 million years, *Quat. Sci. Rev.*, *10*(4), 297–317.

Berger, W. H. (1970), Planktonic foraminifera: Selective solution and the lysocline, *Mar. Geol.*, *8*(2), 111–138.

Blunier, T., and E. J. Brook (2001), Timing of millennial-scale climate change in Antarctica and Greenland during the last glacial period, *Science*, *291*(5501), 109–112.

Blunier, T., et al. (1998), Asynchrony of Antarctic and Greenland climate change during the last glacial period, *Nature*, *394*(6695), 739–743.

Boch, R., H. Cheng, C. Spoetl, R. L. Edwards, X. Wang, and P. Haeuselmann (2011), NALPS: A precisely dated European climate record 120–60 ka, *Clim. Past*, *7*(4), 1247–1259.

Bond, G., W. Broecker, S. Johnsen, J. McManus, L. Labeyrie, J. Jouzel, and G. Bonani (1993), Correlations between climate records from North-Atlantic sediments and Greenland ice, *Nature*, *365*(6442), 143–147.

Broecker, W. S. (1998), Paleocean circulation during the last deglaciation: A bipolar seesaw?, *Paleoceanography*, *13*(2), 119–121, doi:10.1029/97PA03707.
Broecker, W. S., and G. H. Denton (1989), The role of ocean–atmosphere reorganizations in glacial cycles, *Geochim. Cosmochim. Acta*, *53*(10), 2465–2501.
Broecker, W. S., and J. van Donk (1970), Insolation changes, ice volumes and the O^{18} in deep-sea cores, *Rev. Geophys. Space Phys.*, *8*(1), 169–198.
Cacho, I., J. O. Grimalt, C. Pelejero, M. Canals, F. J. Sierro, J. A. Flores, and N. Shackleton (1999), Dansgaard-Oeschger and Heinrich event imprints in Alboran Sea paleotemperatures, *Paleoceanography*, *14*(6), 698–705, doi:10.1029/1999PA900044.
Charles, C. D., and R. G. Fairbanks (1990), Glacial to interglacial changes in the isotopic gradients of Southern Ocean surface water, in *Geological History of the Polar Oceans: Arctic Versus Antarctic*, vol. 308, edited by U. Bleil and J. Thiede, pp. 519–538, Springer, Netherlands.
Charles, C. D., and R. G. Fairbanks (1992), Evidence from Southern-Ocean sediments for the effect of North Atlantic Deep-Water Flux on Climate, *Nature*, *355*(6359), 416–419.
Charles, C. D., J. Lynch-Stieglitz, U. S. Ninnemann, and R. G. Fairbanks (1996), Climate connections between the hemispheres revealed by deep sea sediment core ice core correlations, *Earth Planet. Sci. Lett.*, *142*(1–2), 19–27.
Cheng, H., R. L. Edwards, W. S. Broecker, G. H. Denton, X. G. Kong, Y. J. Wang, R. Zhang, and X. F. Wang (2009), Ice Age Terminations, *Science*, *326*(5950), 248–252.
Chiang, J. C. H., and C. M. Bitz (2005), Influence of high latitude ice cover on the marine Intertropical Convergence Zone, *Clim. Dyn.*, *25*(5), 477–496.
Chiang, J. C. H., M. Biasutti, and D. S. Battisti (2003), Sensitivity of the Atlantic Intertropical Convergence Zone to Last Glacial Maximum boundary conditions, *Paleoceanography*, *18*(4), 1094, doi:10.1029/2003PA000916.
Clark, P. U., A. M. McCabe, A. C. Mix, and A. J. Weaver (2004), Rapid rise of sea level 19,000 years ago and its global implications, *Science*, *304*(5674), 1141–1144.
Crowley, T. J. (1992), North Atlantic deep water cools the Southern Hemisphere, *Paleoceanography*, *7*(4), 489–497, doi:10.1029/92PA01058.
Curry, W. B. (1996), Late Quaternary deep circulation in the Western Equatorial Atlantic, in *The South Atlantic: Present and Past Circulation*, edited by G. Wefer et al., pp. 577–598, Springer-Verlag, Berlin, Heidelberg.
Curry, W. B., and G. P. Lohmann (1986), Late Quaternary carbonate sedimentation at the Sierra-Leone Rise (Eastern Equatorial Atlantic-Ocean), *Mar. Geol.*, *70*(3–4), 223–250.
Cutler, K. B., R. L. Edwards, F. W. Taylor, H. Cheng, J. Adkins, C. D. Gallup, P. M. Cutler, G. S. Burr, and A. L. Bloom (2003), Rapid sea-level fall and deep-ocean temperature change since the last interglacial period, *Earth Planet. Sci. Lett.*, *206*(3–4), 253–271.
Deacon, G. E. R. (1982), Physical and biological zonation in the Southern Ocean, *Deep Sea Res., Part A*, *29*(1), 1–15.
Denton, G. H., T. V. Lowell, C. J. Heusser, C. Schluchter, B. G. Andersen, L. E. Heusser, P. I. Moreno, and D. R. Marchant (1999), Geomorphology, stratigraphy, and radiocarbon chronology of Llanquihue drift in the area of the southern Lake District, Seno Reloncavi, and Isla Grande de Chiloe, Chile, *Geogr. Ann., Ser. A*, *81A*(2), 167–229.
Denton, G. H., W. S. Broecker, and R. B. Alley (2006), The mystery interval 17.5 to 14.5 kyrs ago, *PAGES News*, *14*(2), 14–16.
Denton, G. H., R. F. Anderson, J. R. Toggweiler, R. L. Edwards, J. M. Schaefer, and A. E. Putnam (2010), The Last Glacial Termination, *Science*, *328*(5986), 1652–1656.
Fraile, I., M. Schulz, S. Mulitza, U. Merkel, M. Prange, and A. Paul (2009), Modeling the seasonal distribution of planktonic foraminifera during the Last Glacial Maximum, *Paleoceanography*, *24*, PA2216, doi:10.1029/2008PA001686.
Ganopolski, A., and S. Rahmstorf (2001), Rapid changes of glacial climate simulated in a coupled climate model, *Nature*, *409*(6817), 153–158.
Ganopolski, A., and D. M. Roche (2009), On the nature of lead-lag relationships during glacial-interglacial climate transitions, *Quat. Sci. Rev.*, *28*(27–28), 3361–3378.
Gordon, A. L. (1971), Oceanography of Antarctic waters, in *Antarctic Oceanology I*, Antarctic Research Series, vol. 15, edited by J. L. Reid, pp. 169–203, AGU, Washington, D. C.
Haslett, J., and A. Parnell (2008), A simple monotone process with application to radiocarbon dated depth chronologies, *J. R. Stat. Soc., Ser. C*, *57*(4), 399–418.
Hinnov, L. A., M. Schulz, and P. Yiou (2002), Interhemispheric space-time attributes of the Dansgaard- Oeschger oscillations between 100 and 0 ka, *Quat. Sci. Rev.*, *21*(10), 1213–1228.
Hut, G. (1987), Consultants' Group Meeting on Stable Isotope Reference Samples for Geochemical and Hydrological Investigations: IAEA, Vienna 16–18 September 1985: Report to the Director General, 42 pp., International Atomic Energy Agency, Vienna.
Huybers, P. (2004), Comments on 'Coupling of the hemispheres in observations and simulations of glacial climate change' by A. Schmittner, O. A. Saenko, and A. J. Weaver, *Quat. Sci. Rev.*, *23*(1–2), 207–210.
Huybers, P. (2009), Antarctica's orbital beat, *Science*, *325*(5944), 1085–1086.
Huybers, P., and G. Denton (2008), Antarctic temperature at orbital timescales controlled by local summer duration, *Nat. Geosci.*, *1*(11), 787–792.
Imbrie, J., and J. Z. Imbrie (1980), Modeling the climatic response to orbital variations, *Science*, *207*(4434), 943–953.
Imbrie, J., et al. (1992), On the structure and origin of major glaciation cycles 1. Linear responses to Milankovitch forcing, *Paleoceanography*, *7*(6), 701–738, doi:10.1029/92PA02253.
Imbrie, J., et al. (1993), On the structure and origin of major glaciation cycles 2. The 100,000-year cycle, *Paleoceanography*, *8*(6), 699–735, doi:10.1029/93PA02751.
Jouzel, J., et al. (2007), Orbital and millennial Antarctic climate variability over the past 800,000 years, *Science*, *317*(5839), 793–796.
Kaiser, J., F. Lamy, and D. Hebbeln (2005), A 70-kyr sea surface temperature record off southern Chile (Ocean Drilling Program Site 1233), *Paleoceanography*, *20*, PA4009, doi:10.1029/2005PA001146.
Kaplan, M. R., J. M. Schaefer, G. H. Denton, D. J. A. Barrell, T. J. H. Chinn, A. E. Putnam, B. G. Andersen, R. C. Finkel, R. Schwartz, and A. M. Doughty (2010), Glacier retreat in New Zealand during the Younger Dryas stadial, *Nature*, *467*(7312), 194–197.
Keigwin, L. D., and G. A. Jones (1994), Western North-Atlantic evidence for millennial-scale changes in ocean circulation and climate, *J. Geophys. Res.*, *99*(C6), 12,397–12,410, doi:10.1029/94JC00525.
Keigwin, L. D., W. B. Curry, S. J. Lehman, and S. Johnsen (1994), The role of the Deep-Ocean in North-Atlantic Climate-Change between 70-Kyr and 130-Kyr Ago, *Nature*, *371*(6495), 323–326.
Kennett, J. P., and M. S. Srinivasan (1983), *Neogene Planktonic Foraminifera: A Phylogenetic Atlas*, John Wiley, Hoboken, N. J.
Kim, S.-J., T. J. Crowley, and A. Stössel (1998), Local orbital forcing of Antarctic climate change during the last interglacial, *Science*, *280*(5364), 728–730.
Kindler, P., M. Guillevic, M. Baumgartner, J. Schwander, A. Landais, and M. Leuenberger (2013), NGRIP temperature reconstruction from 10 to 120 kyr b2k, *Clim. Past Discuss.*, *9*(4), 4099–4143.

Kirst, G. J., R. R. Schneider, P. J. Muller, I. von Storch, and G. Wefer (1999), Late Quaternary temperature variability in the Benguela Current System derived from alkenones, *Quat. Res.*, *52*(1), 92–103.
Kissel, C., C. Laj, A. M. Piotrowski, S. L. Goldstein, and S. R. Hemming (2008), Millennial-scale propagation of Atlantic deep waters to the glacial Southern Ocean, *Paleoceanography*, *23*, PA2102, doi:10.1029/2008PA001624.
Knorr, G., and G. Lohmann (2007), Rapid transitions in the Atlantic thermohaline circulation triggered by global warming and meltwater during the last deglaciation, *Geochem. Geophys. Geosyst.*, *8*, Q12006, doi:10.1029/2007GC001604.
Kucera, M., M. Weinelt, T. Kiefer, U. Pflaumann, A. Hayes, M. Weinelt, M.-T. Chen, A. C. Mix, T. T. Barrows, and E. Cortijo (2005), Reconstruction of sea-surface temperatures from assemblages of planktonic foraminifera: Multi-technique approach based on geographically constrained calibration data sets and its application to glacial Atlantic and Pacific Oceans, *Quat. Sci. Rev.*, *24*(7), 951–998.
Lambert, F., M. Bigler, J. P. Steffensen, M. Hutterli, and H. Fischer (2012), Centennial mineral dust variability in high-resolution ice core data from Dome C, Antarctica, *Clim. Past*, *8*(2), 609–623.
Lamy, F., J. Kaiser, H. W. Arz, D. Hebbeln, U. Ninnemann, O. Timm, A. Timmermann, and J. R. Toggweiler (2007), Modulation of the bipolar seesaw in the southeast pacific during Termination 1, *Earth Planet. Sci. Lett.*, *259*(3–4), 400–413.
Landais, A., J. M. Barnola, V. Masson-Delmotte, J. Jouzel, J. Chappellaz, N. Caillon, C. Huber, M. Leuenberger, and S. J. Johnsen (2004), A continuous record of temperature evolution over a sequence of Dansgaard-Oeschger events during Marine Isotopic Stage 4 (76 to 62 kyr BP), *Geophys. Res. Lett.*, *31*, L22211, doi:10.1029/2004GL021193.
Laskar, J., P. Robutel, F. Joutel, M. Gastineau, A. C. M. Correia, and B. Levrard (2004), A long-term numerical solution for the insolation quantities of the Earth, *Astron. Astrophys.*, *428*(1), 261–285.
Le, J. N., and R. C. Thunell (1996), Modelling planktic foraminiferal assemblage changes and application to sea surface temperature estimation in the western equatorial Pacific Ocean, *Mar. Micropaleontol.*, *28*(3–4), 211–229.
LeGrande, A. N., and G. A. Schmidt (2006), Global gridded data set of the oxygen isotopic composition in seawater, *Geophys. Res. Lett.*, *33*, L12604, doi:10.1029/2006GL026011.
Liu, Z., et al. (2009), Transient simulation of Last Deglaciation with a new mechanism for Bolling-Allerod warming, *Science*, *325*(5938), 310–314.
Locarnini, R. A., A. V. Mishonov, J. I. Antonov, T. P. Boyer, H. E. Garcia, O. K. Baranova, M. M. Zweng, and D. R. Johnson (2010), in *World Ocean Atlas 2009, Volume 1: Temperature*, NOAA Atlas NESDIS 68, edited by S. Levitus, 184 pp., U.S. Government Printing Office, Washington, D. C.
Lund, D., J. Adkins, and R. Ferrari (2011), Abyssal Atlantic circulation during the Last Glacial Maximum: Constraining the ratio between transport and vertical mixing, *Paleoceanography*, *26*, PA1213, doi:10.1029/2010PA001938.
Margo_Project_Members (2009), Constraints on the magnitude and patterns of ocean cooling at the Last Glacial Maximum, *Nat. Geosci.*, *2*(2), 127–132.
Martinez-Garcia, A., A. Rosell-Melé, S. L. Jaccard, W. Geibert, D. M. Sigman, and G. H. Haug (2011), Southern Ocean dust-climate coupling over the past four million years, *Nature*, *476*(7360), 312–315.
McManus, J. F., D. W. Oppo, L. D. Keigwin, J. L. Cullen, and G. C. Bond (2002), Thermohaline circulation and prolonged interglacial warmth in the North Atlantic, *Quat. Res.*, *58*(1), 17–21.
McManus, J. F., R. Francois, J. M. Gherardi, L. D. Keigwin, and S. Brown-Leger (2004), Collapse and rapid resumption of Atlantic meridional circulation linked to deglacial climate changes, *Nature*, *428*(6985), 834–837.
Mercer, J. H. (1984), Simultaneous climatic change in both hemispheres and similar bipolar interglacial warming: Evidence and implications, in *Climate Processes and Climate Sensitivity*, Geophysical Monograph Series, vol. 29, edited by J. E. Hansen and T. Takahash, pp. 307–313, AGU, Washington, D. C.
Miller, M., J. Adkins, D. Menemenlis, and M. Schodlok (2012), The role of ocean cooling in setting glacial southern source bottom water salinity, *Paleoceanography*, *27*, PA3207, doi:10.1029/2012PA002297.
Mix, A. C., W. F. Ruddiman, and A. McIntyre (1986), Late Quaternary Paleoceanography of the Tropical Atlantic, 1: Spatial variability of annual mean sea-surface temperatures, 0–20,000 Years Bp, *Paleoceanography*, *1*(1), 43–66, doi:10.1029/PA001i001p00043.
Monnin, E., A. Indermuhle, A. Dallenbach, J. Fluckiger, B. Stauffer, T. F. Stocker, D. Raynaud, and J. M. Barnola (2001), Atmospheric CO_2 concentrations over the last glacial termination, *Science*, *291*(5501), 112–114.
Mortyn, P., C. D. Charles, and D. A. Hodell (2002), Southern Ocean upper water column structure over the last 140 kyr with emphasis on the glacial terminations, *Global Planet. Change*, *34*(3–4), 241–252.
NGRIP_members (2004), High-resolution record of Northern Hemisphere climate extending into the last interglacial period, *Nature*, *431*(7005), 147–151.
Ninnemann, U. S., C. D. Charles, and D. A. Hodell (1999), Origin of global millennial-scale climate events: Constraints from the Southern Ocean deep sea sedimentary record, in *Mechanisms of global climate change at millennial timescales*, Geophysical Monograph, vol. 112, edited by P. U. Clark, R. S. Webb, and L. D. Keigwin, pp. 99–112, AGU, Washington, D. C.
Orsi, A. H., T. Whitworth, and W. D. Nowlin (1995), On the meridional extent and fronts of the Antarctic Circumpolar Current, *Deep Sea Res., Part I*, *42*(5), 641–673.
Pahnke, K., and J. P. Sachs (2006), Sea surface temperatures of southern midlatitudes 0–160 kyr BP, *Paleoceanography*, *21*, PA2003, doi:10.1029/2005PA001191.
Parnell, A. C., J. Haslett, J. R. M. Allen, C. E. Buck, and B. Huntley (2008), A flexible approach to assessing synchroneity of past events using Bayesian reconstructions of sedimentation history, *Quat. Sci. Rev.*, *27*(19), 1872–1885.
Parrenin, F., V. Masson-Delmotte, P. Köhler, D. Raynaud, D. Paillard, J. Schwander, C. Barbante, A. Landais, A. Wegner, and J. Jouzel (2013), Synchronous change of atmospheric CO_2 and Antarctic temperature during the last deglacial warming, *Science*, *339*(6123), 1060–1063.
Peterson, L. C., G. H. Haug, K. A. Hughen, and U. Rohl (2000), Rapid changes in the hydrologic cycle of the tropical Atlantic during the last glacial, *Science*, *290*(5498), 1947–1951.
Petit, J. R., et al. (1999), Climate and atmospheric history of the past 420,000 years from the Vostok ice core, Antarctica, *Nature*, *399*(6735), 429–436.
Piotrowski, A. M., S. L. Goldstein, S. R. Hemming, and R. G. Fairbanks (2005), Temporal relationships of carbon cycling and ocean circulation at glacial boundaries, *Science*, *307*(5717), 1933–1938.
Putnam, A. E. (2013), Warming and glacier recession in the Rakaia valley, Southern Alps of New Zealand, during Heinrich Stadial 1, *Earth Planet. Sci. Lett.*, *382*, 98–110.
Putnam, A. E., G. H. Denton, J. M. Schaefer, D. J. A. Barrell, B. G. Andersen, R. C. Finkel, R. Schwartz, A. M. Doughty, M. R. Kaplan, and C. Schluechter (2010), Glacier advance in southern middle-latitudes during the Antarctic Cold Reversal, *Nat. Geosci.*, *3*(10), 700–704.
Reimer, P. J., M. G. L. Baillie, E. Bard, A. Bayliss, J. W. Beck, P. G. Blackwell, C. B. Ramsey, C. E. Buck, G. S. Burr, and R. L. Edwards (2009), IntCal09 and Marine09 radiocarbon age calibration curves, 0–50,000 years cal BP.

Rind, D., G. Russell, G. Schmidt, S. Sheth, D. Collins, P. deMenocal, and J. Teller (2001), Effects of glacial meltwater in the GISS coupled atmosphere- ocean model - 2. A bipolar seesaw in Atlantic Deep Water production, *J. Geophys. Res.*, *106*(D21), 27,355–27,365, doi:10.1029/2001JD000954.

Roe, G. (2006), In defense of Milankovitch, *Geophys. Res. Lett.*, *33*, L24703, doi:10.1029/2006GL027817.

Ruddiman, W. F., and B. C. Heezen (1967), Differential solution of planktonic foraminifera, *Deep Sea Res., Part A*, *14*, 801–808.

Sachs, J. P., and R. F. Anderson (2005), Increased productivity in the subantarctic ocean during Heinrich events, *Nature*, *434*(7037), 1118–1121.

Schlitzer, R. (2014), Ocean Data View. [Available at http://odv.awi.de].

Schmittner, A., O. A. Saenko, and A. J. Weaver (2003), Coupling of the hemispheres in observations and simulations of glacial climate change, *Quat. Sci. Rev.*, *22*(5–7), 659–671.

Schulz, K., and R. E. Zeebe (2006), Pleistocene glacial terminations triggered by synchronous changes in Southern and Northern Hemisphere insolation: The insolation canon hypothesis, *Earth Planet. Sci. Lett.*, *249*(3), 326–336.

Schulz, M., W. H. Berger, M. Sarnthein, and P. M. Grootes (1999), Amplitude variations of 1470-year climate oscillations during the last 100,000 years linked to fluctuations of continental ice mass, *Geophys. Res. Lett.*, *26*(22), 3385–3388, doi:10.1029/1999GL006069.

Severinghaus, J. P. (2009), CLIMATE CHANGE Southern see-saw seen, *Nature*, *457*(7233), 1093–1094.

Shackleton, N. J. (1974), Attainment of isotopic equilibrium between ocean water and the benthonic foraminifera genus *Uvigerina*: Isotopic changes in the ocean during the Last Glacial, *Colloq. Int. C. N. R. S.*, *219*, 203–209.

Shackleton, N. J., M. A. Hall, and E. Vincent (2000), Phase relationships between millennial-scale events 64,000-24,000 years ago, *Paleoceanography*, *15*(6), 565–569, doi:10.1029/2000PA000513.

Shakun, J. D., P. U. Clark, F. He, S. A. Marcott, A. C. Mix, Z. Liu, B. Otto-Bliesner, A. Schmittner, and E. Bard (2012), Global warming preceded by increasing carbon dioxide concentrations during the last deglaciation, *Nature*, *484*(7392), 49–54.

Siddall, M., E. J. Rohling, A. Almogi-Labin, C. Hemleben, D. Meischner, I. Schmelzer, and D. A. Smeed (2003), Sea-level fluctuations during the last glacial cycle, *Nature*, *423*(6942), 853–858.

Sima, A., A. Paul, and M. Schulz (2004), The Younger Dryas - An intrinsic feature of late Pleistocene climate change at millennial timescales, *Earth Planet. Sci. Lett.*, *222*(3–4), 741–750.

Singer, B. S., H. Guillou, B. R. Jicha, C. Laj, C. Kissel, B. L. Beard, and C. M. Johnson (2009), $^{40}Ar/^{39}Ar$, K-Ar and ^{230}Th-^{238}U dating of the Laschamp excursion: A radioisotopic tie-point for ice core and climate chronologies, *Earth Planet. Sci. Lett.*, *286*, 80–88, doi:10.1016/j.epsl.2009.06.030.

Skinner, L. C., S. Fallon, C. Waelbroeck, E. Michel, and S. Barker (2010), Ventilation of the deep Southern Ocean and deglacial CO_2 rise, *Science*, *328*(5982), 1147–1151.

Sowers, T., and M. Bender (1995), Climate records covering the last deglaciation, *Science*, *269*(5221), 210–214.

Steig, E. J., and R. B. Alley (2002), Phase relationships between Antarctic and Greenland climate records, *Ann. Glaciol.*, *35*, 451–456.

Stenni, B., et al. (2011), Expression of the bipolar see-saw in Antarctic climate records during the last deglaciation, *Nat. Geosci.*, *4*(1), 46–49.

Stocker, T. F., and S. J. Johnsen (2003), A minimum thermodynamic model for the bipolar seesaw, *Paleoceanography*, *18*(4), 1087, doi:10.1029/2003PA000920.

Stoner, J. S., C. Laj, J. E. T. Channell, and C. Kissel (2002), South Atlantic and North Atlantic geomagnetic paleointensity stacks (0–80 ka): Implications for inter-hemispheric correlation, *Quat. Sci. Rev.*, *21*(10), 1141–1151.

Stott, L., A. Timmermann, and R. Thunell (2007), Southern hemisphere and deep-sea warming led deglacial atmospheric CO2 rise and tropical warming, *Science*, *318*, 435–438.

Stroeve, J. C., M. C. Serreze, M. M. Holland, J. E. Kay, J. Malanik, and A. P. Barrett (2012), The Arctic's rapidly shrinking sea ice cover: A research synthesis, *Clim. Change*, *110*(3–4), 1005–1027.

Stuiver, M., and P. J. Reimer (1993), Extended ^{14}C data-base and revised Calib 3.0 ^{14}C age calibration program, *Radiocarbon*, *35*(1), 215–230.

Svensson, A., K. K. Andersen, M. Bigler, H. B. Clausen, D. Dahl-Jensen, S. M. Davies, S. J. Johnsen, R. Muscheler, F. Parrenin, and S. O. Rasmussen (2008), A 60 000 year Greenland stratigraphic ice core chronology, *Clim. Past*, *4*(1), 47–57.

Thornalley, D. J. R., S. Barker, J. Becker, G. Knorr, and I. R. Hall (2013), Abrupt changes in deep Atlantic circulation during the transition to full glacial conditions, *Paleoceanography*, *28*, 253–262, doi:10.1002/palo.20025.

Timmermann, A., U. Krebs, F. Justino, H. Goosse, and T. Ivanochko (2005), Mechanisms for millennial-scale global synchronization during the last glacial period, *Paleoceanography*, *20*, PA4008, doi:10.1029/2004PA001090.

Timmermann, A., et al. (2007), The influence of a weakening of the Atlantic meridional overturning circulation on ENSO, *J. Clim.*, *20*(19), 4899–4919.

Timmermann, A., O. Timm, L. Stott, and L. Menviel (2009), The roles of CO_2 and orbital forcing in driving Southern Hemispheric temperature variations during the last 21 000 Yr, *J. Clim.*, *22*(7), 1626–1640.

Toggweiler, J. R., J. L. Russell, and S. R. Carson (2006), Midlatitude westerlies, atmospheric CO_2, and climate change during the ice ages, *Paleoceanography*, *21*, PA2005, doi:10.1029/2005PA001154.

Vellinga, M., and R. A. Wood (2002), Global climatic impacts of a collapse of the Atlantic thermohaline circulation, *Clim. Change*, *54*(3), 251–267.

Veres, D., L. Bazin, A. Landais, H. Toyé Mahamadou Kele, B. Lemieux-Dudon, F. Parrenin, P. Martinerie, E. Blayo, T. Blunier, and E. Capron (2012), The Antarctic ice core chronology (AICC2012): An optimized multi-parameter and multi-site dating approach for the last 120 thousand years, *Clim. Past Discuss.*, *8*(6), 6011–6049.

Waelbroeck, C., L. Labeyrie, E. Michel, J. C. Duplessy, J. F. McManus, K. Lambeck, E. Balbon, and M. Labracherie (2002), Sea-level and deep water temperature changes derived from benthic foraminifera isotopic records, *Quat. Sci. Rev.*, *21*(1–3), 295–305.

WAIS_Divide_Project_Members (2013), Onset of deglacial warming in West Antarctica driven by local orbital forcing, *Nature*, doi:10.1038/nature12376.

Wang, X. F., A. S. Auler, R. L. Edwards, H. Cheng, P. S. Cristalli, P. L. Smart, D. A. Richards, and C. C. Shen (2004), Wet periods in northeastern Brazil over the past 210 kyr linked to distant climate anomalies, *Nature*, *432*(7018), 740–743.

Wang, Y. J., H. Cheng, R. L. Edwards, Z. S. An, J. Y. Wu, C. C. Shen, and J. A. Dorale (2001), A high-resolution absolute-dated Late Pleistocene monsoon record from Hulu Cave, China, *Science*, *294*(5550), 2345–2348.

Weldeab, S., D. W. Lea, R. R. Schneider, and N. Andersen (2007), 155,000 years of West African monsoon and ocean thermal evolution, *Science*, *316*(5829), 1303–1307.

Weyl, P. K. (1968), The role of the oceans in climatic change: A theory of the ice ages, in *Meteorological Monographs*, *8*(30), 37–62.

Woillard, G. (1979), Abrupt end of the last interglacial s.s. in north-east France, *Nature*, *281*, 558–562.

Wolff, E. W., H. Fischer, and R. Rothlisberger (2009), Glacial terminations as southern warmings without northern control, *Nat. Geosci.*, *2*(3), 206–209.

Wunsch, C. (2003), Greenland - Antarctic phase relations and millennial time-scale climate fluctuations in the Greenland ice-cores, *Quat. Sci. Rev.*, *22*(15–17), 1631–1646.

Wüst, G., W. Brogmus, and E. Noodt (1954), Die zonale Verteilung von Salzgehalt, Niederschlag, Verdunstung, Temperatur und Dichte an der OberflÃ¤che der Ozeane, *Kiel. Meeresforsch.*, *10*(1954), 2.

Zhang, X., G. Lohmann, G. Knorr, and X. Xu (2013), Different ocean states and transient characteristics in Last Glacial Maximum simulations and implications for deglaciation, *Clim. Past*, *9*, 2319–2333, doi:10.5194/cp-9-2319-2013.

Ziegler, M., E. Tuenter, and L. J. Lourens (2010), The precession phase of the boreal summer monsoon as viewed from the eastern Mediterranean (ODP Site 968), *Quat. Sci. Rev.*, *29*(11–12), 1481–1490.